Title: Chronic spinal injury repair by olfactory bulb ensheathing glia and feasibility for autologous therapy

Running title: Chronic spinal injury repair by adult OEG

This work was supported by the Ministry of Health (grant 01/1134), Ministry of Education and Science (SAF2004-04773), Fundación Investigación en Regeneración del Sistema Nervioso and the National Institutes of Health (Grant R01NS054159-01, subaward 0845 G GD202).

Authors:

Cintia Muñoz-Quiles[1,2], Fernando F. Santos-Benito[1], M. Beatriz Llamusí[1,2] and Almudena Ramón-Cueto[1] *

[1] Laboratory of Neural Regeneration, Institute of Biomedicine, Spanish National Research Council (CSIC), Jaime Roig 11, 46010 Valencia, Spain.

[2]Fundación Investigación en Regeneración del Sistema Nervioso, Artes y Oficios 39, 46021 Valencia, Spain.

* Corresponding author.

Published in:

Journal of Neuropathology and Experimental Neurology, Dec 2009; Vol 68 (12); pp 1294-1308

Impact factor: 5,140

Quartile 1: 7% in the area of Pathology and 14% in Neurosciences

SUMMARY

Olfactory Bulb Ensheathing Glia (OB-OEG) promote spinal cord injury (SCI) repair in rats after transplantation at acute or subacute stages (up to 45 days). However, the most realistic clinical scenario is the chronic, in which no more cellular and molecular changes take place at the injury, and this occurs beyond the third month in rodents. Whether adult OB-OEG grafts promote repair of severe chronic SCI has not been previously addressed. Rats with complete SCI that were transplanted 4 months after injury exhibited a progressive improvement in motor function and axonal regeneration from different brainstem nuclei across and beyond the SCI site. A positive correlation between motor outcome and axonal regeneration suggested a role for brainstem neurons in the recovery. Functional and histological outcomes did not differ after transplantation at subacute or chronic stages. Thus, autologous transplantation is a feasible approach as there is a time-frame for patient stabilization and OEG preparation; moreover, the healing effects of OB-OEG on established injuries may offer new therapeutic opportunities for chronic SCI patients.

Key words: axonal regeneration, chronic transplantation, paraplegia, glial scar, functional recovery.

INTRODUCTION

Most spinal cord injuries (SCI) cause permanent and irreversible functional deficits in patients. The devastating prognosis for people suffering severe SCI has provided an impetus to search for therapies aimed at curing this chronic pathology and olfactory ensheathing glia (OEG) transplantation is a promising repair strategy. There are more than 40 articles showing positive effects of OEG after SCI of various types and severities (reviewed in (1)), most after spinal cord trauma, (2-9) including contusion (10), but there are 13 articles showing no or limited beneficial effects. The differences seem related to the sources of cells, the ages of the animals and the methods used for culture and transplantation. After the third week in vitro, adult rodent OB-OEG become senescent with an associated change in phenotype (11). Thus, grafting of older cultures may compromise cell survival and/or migration (12-15). Whether to use OEG from the olfactory bulb (central) or from the epithelium (peripheral) is also a debated issue. Mucosally derived OEG are more accessible, but they seem to have inferior migratory and growth-promoting properties (16-18) compared with bulbar OEG (2-9). Based on these studies and the prospect for autologous therapy, we have used adult nonsenescent OEG of bulbar origin in this study.

In most of the previous studies, OEG have been transplanted immediately after SCI (acute stage). Because many patients take several weeks or even months for clinical stabilization, however, a delayed transplant paradigm would be more clinically relevant. Moreover, if autologous transplantation is to be used, cell preparation requires time. Hence, an intervention several months after SCI is a more realistic paradigm. Experimental OB-OEG grafting has been delayed for 7 and 30 days (10, 19) but never beyond 45 days (20); which has been considered to be the subacute stage (21, 22). SCI are considered to be at the chronic stage when, in the absence of further manipulation,

no more cellular and molecular changes occur, which is after the third month in rodents (21, 22). Here, we determine the repair efficacy of OB-OEG grafted at the chronic stage into the injury site after complete SCI to evaluate real axonal regeneration rather than plasticity of spared fibers. We also compared functional and histological outcomes with grafting at the subacute stage and quantified the regeneration of relevant descending motor tracts at both subacute and chronic stages.

METHODS

The experimental procedures adhered to the recommendations of the European Union and the US Department of Health for the care and use of laboratory animals and were approved by the Ethics Committee of our institution.

OEG cultures from adult olfactory bulbs

OB-OEG primary cultures were obtained from the first two olfactory bulb layers of 2- to 2.5- month-old Wistar Hannover rats (Harlan Laboratories, Barcelona, Spain). Seven days after plating, p75 receptor-expressing OB-OEG were purified as reported previously (2, 11). They were cultured in D/F-10S (1:1 DEMEM:Ham's F-12, Gibco-Invitrogen, Madrid, Spain; 10% fetal bovine serum), at 37ºC, 5% CO_2. At 2 days after purification, 2 μM forskolin (Sigma-Aldrich Química, Madrid, Spain) and 20 μg/ml bovine pituitary extract (Biomedical Technologies Inc., Stoughton, MA) were added. Pure p75-OEG were expanded for less than 2 weeks to avoid senescence (11). Cells were detached from the flasks, labeled with bisbenzimide (Hoechst 33342; Sigma) and transplanted at a density of 100,000 cells/μl in DMEM as performed previously (2, 4, 23, 24).

Surgery and OB-OEG transplantation

Twenty-eight adult female Wistar Hannover rats (2.5-3 months of age, 200-230 grams, n=28) were anesthetized with isofluorane and N_2:O_2 (40:60) and a laminectomy to expose T8 to T9 segments performed. In 22 of the animals, the dura was opened and the spinal cords completely sectioned using microscissors. The stumps were lifted to ensure completeness of the lesion (Fig. 1A) (4).

The paraplegic animals were then divided into 3 groups: i) subacute (SA), ii) Chronic (Chr) and iii) Non-transplanted (Non-T). The SA rats (n=5) were transplanted with p75 OB-OEG at 1 month after injury and Chr rats (n=5) at 4 months after SCI. Non-T animals (n=12) were not transplanted but injected with DMEM after 1 (n=6) and 4 months (n=6). Six more animals were not transected (sham-operated group) and received a second surgery after 1 (n=3) and 4 months (n=3). In the second surgery, we removed the connective tissue formed underneath the resin bridge and above the spinal cord (Fig. 1D) to expose the injury region. Glial and fibrous scars, created between the spinal cord stumps, were not removed (Fig. 1E). The OB-OEG were stereotaxically grafted into both, caudal and rostral intact spinal cord stumps, at 1mm from the stump border, as previously described (4, 23) (Fig. 1F). Cells were injected in the midline of each stump, from ventral to dorsal, into 4 sites at 1.3, 1.0, 0.8 and 0.5 mm respectively. Each site received 0.5 µl of 50,000 OEG (200,000 per stump). Non-T animals were injected with 0.5 µl of DMEM instead, and shams were not injected.

In both surgeries, spinal cords were covered with durafilm (Ferrosan, London, UK). Vertebral columns were stabilized placing a resin bridge between adjacent vertebrae (Fig. 1C), made of an autopolymerizing acrylic resin (DuraLay; Reliance, Dental Manufacturing. Co. worth, IL) (25) (26).

Animal care, physiotherapy and rehabilitation

Immediately after surgery, rats received 1 ml of Ringer´s lactate solution and analgesic magnesium metamizol (Nolotil, Boeringer Ingelheim, Barcelona, Spain) subcutaneously. An antibiotic, Augmentine (amoxiciline/clavulanic acid, 1g/200mg, GlaxoSmithKline, Madrid, Spain), was also administered and twice more every 8 hours. Urinary bladder was manually expressed 4 times a day until autonomous voidance and then once daily. Detailed postoperative care has been described (27). To keep paraplegic rats in good condition they received active and passive ROM (range of motion). Active ROM was performed using the climbing test once a week (Appendix 1). Daily passive ROM included movement of joints below the level of injury (25 times each joint) and massages of muscles and skin over bone prominences.

All animals were allowed to survive for 12 months after the first surgery (lesion surgery) and subjected to a third surgery for tracer injection (see below). All paraplegic animals with complete lesion had to be maintained in good and stable clinical condition for 1 year. After paraplegia, animals had 2 additional surgeries, one for OB-OEG transplantation and another for tracer injection. At the time of the last surgery, the animals were not only paraplegic but also aged (15 months old). Animal care protocols were adapted from those used for humans (27).

Functional Analysis

A detailed description of the climbing test used in this study was previously reported (4), is described in Appendix 1 and presented as Supplemental data (Video, Supplemental Digital Content 1, http://links.lww.com/NEN/A62). Training started when animals were 1 month old and continued until the first surgery. Comparison of the

performance of transplanted and non-transplanted rats started 1 month after the first surgery (lesion) (Fig 2).

Tracer injection

At 12 months after lesion, all animals underwent a third surgery for tracer injection. A cocktail of 25% Horseradish Peroxidase (HRP) and 5% wheat germ agglutinin (WGA)-HRP (Sigma-Aldrich Química, Madrid, Spain) in 0.9% NaCl was injected stereotaxically into the caudal stump, at 0.5 cm from its edge as before (3). Briefly, peroxidise was injected into 13 sites (0.1µl /site) ventrodorsally in the midline (5 injections) and at 0.8 mm to the left and right (4 injections in each side) at 2, 1.6, 1.2, 0.8, and 0.4 mm in the midline; 1.6, 1.2, 0.8, 0.4 mm in left and right sides. Rats were allowed to survive 48 hours before perfusion. This retrograde tracer is endocytosed by axons either passing through or terminating at the site of injection and hence, by axons regenerating at least 0.5 cm beyond the lesion.

Histological processing

Animals were perfused with 4% paraformaldehyde; the spinal cords and brainstems were dissected and post-fixed for 5 hours. Coronal sections of the brainstems and longitudinal sagittal sections of the spinal cords were obtained in a cryostat (-20ºC, 20 µm sections). Consecutive sections of the whole structures were collected onto different slides and processed for peroxidise detection and immunohistochemistry.

Peroxidase detection

We sectioned the entire brain stem (20 µm sections) and collected all sections sequentially in order to locate each section within the brain stem. For peroxidase

detection, equally spaced sections (100 μm) were processed through the entire brainstem. In these sections, the cytoplasms of Peroxidase-traced somata were detected with the chromogen diaminobenzidine (DAB, Vector Laboratories, Burlingame, CA). To increase the signal, sections were also labelled with an antibody against wheat germ agglutinin (anti-WGA, Vector, 1/250, overnight at 4ºC) and a biotinylated-conjugated secondary antibody (Vector Laboratories, Burlingame, CA) (1/200, 45 min), then incubated with Vectastain Elite ABC Kit Standard from Vector as indicated by manufacturer. Spinal cord sections of 3 animals per group (n=9) were also processed as described above in order to determine whether peroxidase diffused beyond the injury region (Figure, Supplemental Digital Content 2, http://links.lww.com/NEN/A63)

Immunohistochemical labelling of the spinal cord

We labelled spinal cord sections containing the entire injury region and 2 segments above and below (i.e. from T6 to T10). Because the sections were collected sequentially, we could identify the precise location of each section within the cord. Depending on the type of analysis (see below), these sections were incubated overnight at 4ºC with the following primary antibodies: polyclonal rabbit anti-glial Fibrillary Acidic Protein (GFAP, Dako, Barcelona, Spain; 1/500) to label reactive astroglia and to delimit the glial scar; monoclonal mouse anti-Neurofilament (NFL, Hybridoma Bank RT 97, Iowa City, Iowa; 1/1500) to stain axons; and polyclonal rabbit anti-Rat S100 (Dako, Barcelona, Spain; 1/100) to distinguish OEG. The following day, sections were incubated with the respective secondary antibodies conjugated with Texas Red (Jackson Immunoresearch, West Grove, PA; 1/500) or Oregon Green (Molecular Probes-Invitrogen, Barcelona, Spain; 1/500), for 45 min at room temperature. Labeled sections were mounted with Fluoromount (SouthernBiotech, Birmingham, AL) and coverslipped.

Quantification methods at the injury site

Quantification of tissue degeneration

Every fifth section of the entire spinal cord separated by100 μm was analysed (28 sections per rat). Fibrous scar and cavities, a direct consequence of tissue degeneration, are GFAP negative and were quantified by measuring the volume of GFAP-negative tissue at the injury site. In each GFAP-labelled section we digitalized the lesion area using a Leica microscope. In each section, fibrous scar and cystic areas (GFAP negative tissue) were outlined and measured (μm^2) using the image analysis program Metamorph, and the volume calculated as previously described (28, 29). Briefly, individual "subvolumes", which correspond to the area in 1 section multiplied by the distance to the next (100 μm), were summed.

Quantification of axons

Twenty eight sections adjacent to those used for the quantification of tissue degeneration (also separated 100 μm) were double stained with anti-GFAP to define the borders of the GFAP positive glial scar and with anti-NFL to detect axons. Quantification was done within the GFAP negative fibrous scar. From the total number of pixels in this region determined by image analysis, the percentages of those showing anti-NFL labelling were calculated. The averages of the percentages per rat were used for group comparisons. We used the image analysis program Metamorph.

Quantification of neuronal regeneration

Every fifth section of the whole brainstem was used for quantifying the number of peroxidase-traced neurons. Because sections were collected in order, the precise location within the brain stem of each section was known. For nuclei identification we followed Patxinos and Watson atlas (30). A distance between sections of 100 μm

avoided double/triple counting the same neuron in adjacent sections and, hence, false positive counts. Peroxidase-containing somata were identified by the cytoplasmic brown DAB chromogen reaction. We counted the total number of labelled cell bodies in the locus coeruleus, reticular formation, raphe, vestibular and red nucleus using a Leica microscope. Sections used for counting in each nucleus, and per rat, were the following: i) red nucleus: 14 (left) and 14 (right); ii) Reticular formation: 66; iii) locus coeruleus: 20 (left) and 20 (right); iv) vestibular nucleus: 26 (left) and 26 (right); v) raphe nucleus: 60. Images of sections were taken at 10x magnification using a camera (Leica DFC300 FX) attached to the microscope.

Statistical Analysis

The variables of the behavioural recovery study were ordered categories (31). Each climbing grid was placed at an increasing angle from the horizontal plane and, thus, has a higher slope than the previous (45º<60º<75º<90º). Each slope correlates with one level of difficulty for the animals. We assigned scores to each ordinal category or slope and named them "climbing levels" (1<2<3<4). For ordinal categories, non-parametric Kruskal-Wallis and Mann-Withney U tests are most appropriate (32). We used the former test to compare the ability of the non-T, OEG-transplanted and Sham groups to climb the 4 different climbing levels at both SA and Chr stages. Post hoc "Conover-Inman was used for pairwise comparisons (33). Mann-Whitney U test was used to compare the ability to succeed in the climbing test of non-T versus OEG-transplanted groups, also at both, SA and Chr stages. We also used Kruskal-Wallis to evaluate the significance of the time-dependent improvement in function observed within the same group and between groups. Statistical analyses of differences between groups in the number of regenerated neurons (total and nuclei by nuclei) and the extent

of tissue degeneration at the injury site were also made by nonparametric Kruskal-Wallis and Mann-Whitney tests. Non-parametric statistics were used because the experimental groups had fewer than 10 animals. Data are presented as the mean $\pm$ SEM. In all cases, differences were considered significant if $p < 0.05$. Linear regression analysis was used to evaluate the correlation between the functional recovery and the number of neurons regenerating axons from individual animals.

For an estimation of the temporary progression of the functional recovery per rat, a score for each animal was calculated by summing the level achieved in the climbing test at each month during the testing period. The scores obtained were also correlated by linear regression with the number of regenerated neurons from individual animals.

RESULTS

All animals survived following injury and after the following 2 surgeries (transplantation and tracer injection), except for 1 Non-T rat that died during the second surgery (DMEM injection); 4 more Non-T rats died, respectively, at 1, 1.5, 2 and 4 months after the second surgery because of autonomic dysreflexia or unknown causes. One Non-T rat was eliminated from the study because it developed autotomy of its hind limb. Thus, 6 rats were used as Non-T controls. Strikingly, none of the OB-OEG grafted rats presented any complication and just 1 animal from the Chr group died at the very end of the study (11.5 months after injury).

OB-OEG-transplantation improved voluntary hindlimb movement

All transplanted and non-T SCI animals presented flaccid hindlimb paralysis. We started to test the climbing ability of all animals 1 month after lesion. During the whole period, Non-T rats of either group (second surgery after 1 or 4 months) did not

show any difference in the performance ($p = 0.794$ and $p = 0.770$, respectively). This is in agreement with previous studies showing the absence of histological differences after culture medium injection (10). In addition, in our case, this indicates that the second surgery and our injection protocol were innocuous and did not interfere with the normal progression of the pathology. Because all paraplegic Non-T rats were not statistically different, they were considered as a single group ($n = 6$).

Rats from both SA and Chr groups behaved as Non-T rats in the climbing test before transplantation. We started comparing the climbing behaviour of OB-OEG grafted and non-grafted rats from the first month post-grafting which corresponds to the second month post-lesion for the SA group and the fifth for the Chr (Fig. 3C).

Functional recovery after grafting at the subacute stage

All SA transplanted rats succeeded in performing the climbing test (fig 3A). There was a significant functional improvement of SA group in the ability to climb with respect to the non-T group ($p < 0.001$). The OB-OEG grafted rats showed a progressive improvement in climbing abilities and from the second month after transplantation, differences between SA and Non-T rats became evident. At this time, 2 (40%) out of 5 SA rats achieved level 1. A month later, one of these rats improved up to level 2, and a third reached level 1. At 5 months postgrafting, all SA rats succeeded in the climbing test: 1 achieved level 3 and 4 (80%) reached level 1. By comparison, half of Non-T rats (50%) failed to perform any climbing level. Although the remaining exhibited some spontaneous improvement, the recovery of Non-T rats was never comparable with that of transplanted animals. Only 1 of 6 Non-T rats overcame level 1 at the second month post-injury and was the only one improving thereafter. After the fourth and fifth months, respectively, another 2 rats achieved the lowest climbing level, but with no further improvement (Fig. 3A). By comparison, SA animals presented better scores in

the climbing test, with statistical significance, and continued improving function after the fifth month. At 7 months after OB-OEG transplantation, SA rats reached their maximum functional recovery, 4 of them (80%) achieving level 3, and 1 level 2 (Fig. 3A). A monthly comparison of functional outcome showed significant differences between SA and Non-T groups from the sixth month after transplantation until the end of the experiment. Conover-Inman post hoc values were $p = 0.0145$ at the sixth month and $p = 0.0095$ at the seventh month. Mann-Whitney U test also showed a significance of $p = 0.029$ at month six and $p = 0.020$ at month seven and later. After the fifth month post-grafting, the climbing performance exhibited by OB-OEG transplanted rats was better than at the first ($p = 0.004$) and second months ($p = 0.042$). This time-dependent recovery was improved further at seventh month. Climbing performance at seventh month was significantly better than that at first ($p = 0.004$), second ($p = 0.006$) and third and fourth months ($p = 0.009$, both). By comparison, Non-T animals did not improve their climbing abilities with time and the spontaneous outcome exhibited by some of them did not have statistical significance.

Functional recovery after grafting at the chronic stage

Before transplantation, Chr rats behaved in the climbing test similar to Non-T rats. After transplantation (4 months after injury) they recovered function more than Non-T rats ($p = 0.002$). One Non-T and 2 Chr rats showed some spontaneous recovery just before the second surgery (4 months post-lesion) by achieving the lowest climbing level (not shown). The functional capabilities of the 2 Chr rats showing some recovery were not diminished after OB-OEG injection, suggesting a proper integration of the graft within the cord parenchyma and indicating that our transplantation can be performed safely after a chronic SCI.

The Chr rats improved motor function significantly more than Non-T rats (p=0.002) and improvement was progressive (p=0.016) (Fig. 3B). The Chr rats had improved motor function 2 months (6 post-lesion) after grafting. At this period 3 rats achieved level 1 and, a month later, they had improved to level 2 or to level 3. All Chr rats were able to climb at least level 1 at 4 months after grafting. At the fifth month, 3 out of 5 rats were able to achieve level 3, 1 achieved level 2, and the other level 1. These animals gained their maximum functional recovery after the seventh month and this was significantly different from the maximum climbing performance achieved by Non-T rats (Conover-Inman p = 0.0299, Mann-Whitney U test p = 0.045). The level of recovery of the Chr rats observed was statistically higher at 4 months post-grafting than at 1 (p = 0.021) and 2 months (p = 0.033). These differences remained significant and increased further at the seventh month (p = 0.013 *vs* month 1; p = 0.016 *vs* month 2) (Fig. 3C).

Comparison between OB-OEG-transplanted groups at subacute and chronic stages

Despite the transplantation delay (1 or 4 months), SA and Chr rats started recovering motor function after the second month post-grafting and continued doing so during the following months. There were no differences in climbing performance at any month post grafting (p between 0.1 and 0.635) reaching the maximum at seventh month. All OB-OEG transplanted rats presented movement of the hindlimbs, plantar placement of the paws and body weight support, necessary to succeed in the test, independent of the stage of transplantation (n = 10). At the end of the study, regardless of the transplantation delay, 70% of all OEG grafted rats were able to reach the platform by climbing from level 3, 10% climbing from the level 2 and 20% from level 1. All (100%) rats from SA and Chr groups had accomplish the climbing test by the fifth and fourth

months respectively. At these post-grafting testing periods the climbing performance significantly exceeded the previous test period ($p = 0.004$ and $p = 0.021$ respectively).

Tissue repair after SCI by OB-OEG grafts

Evaluation of transplantation effects on scarring

Macroscopically, in all transplanted rats there was a white and opaque tissue at the injury site bridging both cord stumps (Fig. 4A and B), suggesting some quantitative differences in the tissue. This property was not observed in Non-T animals. Instead, the bridge region appeared thin and translucent (Fig. 4C). By microscopy, all injured spinal cords showed an interruption of GFAP immunolabelling at the lesion, over the entire spinal cord width, indicating that transection was complete (Fig. 5).

The Hoechst dye was not transferred from OB-OEG to cells of the host spinal cords (Appendix 2; Figure, Supplemental Digital Content 3, http://links.lww.com/NENA64). The distribution of OB-OEG within the spinal cord was the same as previously described after transplantation at the acute stage (3, 4). Briefly, OB-OEG migrated from the injection sites and invaded the glial and fibrous scars. They intermingled with reactive astrocytes and the inhibitory fibrous scar did not hinder their migration Figure, Supplemental Digital Content 3, http://links.lww.com/NENA64). To quantify the effect of OB-OEG on tissue repair and scarring, we calculated the volume of GFAP-negative tissue (fibrous scar) and cavities formed between GFAP positive stumps (Fig. 5). Both volumes (fibrous scar and cavities) were added together as they provide a measure of trauma-induced degeneration (see methods). The mean volume of GFAP negative tissue was larger in Non-T group (4.93 ± 0.96 mm^3) as compared with SA (2.42 ± 0.34 mm^3, $p = 0.009$) and Chr (2.14 ± 0.57 mm^3, $p = 0.05$ for Chr) groups (Fig. 5). Therefore, the amount of fibrosis and

necrosis was double in non-grafted spinal cords with respect to OB-OEG containing ones. This indicates that OB-OEG favoured either the formation of new tissue and better stump healing and/or the decrease of tissue loss in the case of SA rats, thereby helping spinal cord repair at the lesion site. There were not significant differences in the values between rats transplanted at SA and Chr stages ($p = 0.624$). Thus, the efficacy of OB-OEG in spinal cord preservation at the injury appears to be maintained independently of the timing of transplantation. The volume of GFAP negative tissue (fibrosis and cysts) was inversely related to the maximum functional levels in the climbing test ($r = -0.800$; $p < 0.001$). Therefore, better tissue preservation in OB-OEG grafted rats seemed to help axonal regeneration across the lesion.

OB-OEG promotes axonal regeneration of brainstem neurons beyond the scar

Axons unable to cross tend to sprout more profusely in the scar than axons elongating straight beyond. Consequently, nontreated animals may have more fibers within the scar than animals showing axonal regeneration. Although this makes NFL labeling at the scar not a very accurate method for quantification of axonal regeneration, we wanted to have an estimation of the number of fibers invading the injury region. We observed NFL-immunolabeled axons entering the scars in both OB-OEG grafted and Non-T spinal cords. There were no group differences in the number of pixels representing NFL positive sprouts within the scar tissue of SA, Chr and Non-T rats ($p = 0.462$).

To quantify axonal regeneration beyond the lesion, we injected the retrograde tracer at 0.5 cm from the rostral border of the caudal stump. We observed no inadvertent leakage or spread of the tracer rostrally into the lesion, by analysing microscopically the spinal cords of 3 animals from each group. The retrograde tracer

did not reach the injury site or the edge of the caudal stump, but instead remained within the caudal cord Figure, Supplemental Digital Content 2, http://links.lww.com/NENA63). Because the tracer was injected at 0.5 from the lesion, only axons crossing the injury region, invading the caudal stump and growing at least 0.5 cm beyond could pick up the tracer Thus, all neurons containing peroxidase were regenerating neurons whose axons grew 0.5 cm or more far down into the caudal stump. Retrogradely peroxidase-labelled neurons were counted in 5 brainstem nuclei relevant for the initiation and modulation of locomotor patterns: reticular formation, locus coeruleus, vestibular, raphe and red nucleus. All nuclei examined contained HRP-labelled neurons (Fig. 6). The mean total number of peroxidase-labelled neurons in the brainstem of sham rats was 16,399 ± 609 (n = 3). This value was 5,203 ± 1,116 in SA rats and 6,330 ± 1,176 in Chr group. The total number of neurons regenerating their axons beyond the lesion was more than twice in OB-OEG grafted animals (either SA or Chr) compared to Non-T rats (2,198 ± 416) and this was statistically significant ($p < 0.018$) (Fig. 7). Significance was greater when analysis was performed comparing individual nuclei: Reticular formation (SA: $p = 0.006$; Chr: $p = 0.011$), vestibular nucleus (SA: $p = 0.018$; Chr: $p = 0.019$), locus coeruleus (SA: $p = 0.018$; Chr: $p = 0.033$), red nucleus (SA: $p = 0.018$; Chr: $p = 0.011$) and raphe (SA: $p = 0.201$; Chr. $p = 0.019$). The only exception was raphe nucleus of the SA group, in which differences were not significant. The Chr rats exhibited greater numbers of regenerating brainstem neurons in all analysed nuclei than SA rats, but differences between the transplantation paradigms were not significant. The percentage of total traced neurons, per nuclei and experimental group, with respect to equivalent nuclei of sham animals (100 %) was 38.6% and 31.7% in Chr and SA, respectively. By comparison 13.4% of neurons of the Non-T rats were labeled. Raphe and red nuclei contained the highest number of

regenerating neurons in both SA and Chr groups. The SA rats presented 63.4% and 46.6% of neurons traced in raphe and red nuclei respectively, and the Chr rats showed 58.2% and 46.9%. Interestingly, in Non-T animals, the raphe and red nuclei showed more spontaneous regeneration than other nuclei with 25.9% neurons labelled in raphe and 28.9% in the latter. The highest incidence of regenerating neurons after OB-OEG grafting (up to eight fold) was observed in the locus coeruleus (19% in Chr; 13.8% in SA, compared to 2.4% in Non-T). The percentage of peroxidase-labelled neurons in the reticular formation and vestibular nuclei of transplanted rats compared to sham animals was 30 to 40 %, respectively; three times more than in Non-T group (Table).

In summary, the histological results show that axons from several brainstem nuclei that arer relevant to motor function were able to cross the scars and grow beyond into the caudal stump. The extent of axonal regeneration was similar in rats transplanted at SA and Chr phases, indicating that the repair efficacy of OB-OEG remained unaltered after delayed transplantation and was independent of the stage of the healing process. Moreover, brainstem neurons retained their capacity to respond positively to OB-OEG up to 4 months post-lesion. Therefore, there is a window of at least 4 months in which OB-OEG could be applied without any apparent adverse effect.

Functional outcome correlated with the extent of axonal regeneration and tissue preservation.

The maximum climbing level achieved by each rat was positive correlated with total number of retrogradely labeled brainstem neurons ($r = 0.733$; $p = 0.001$). There was also a correlation between climbing ability and the number of somata in each independent nucleus and in all nuclei analyzed (r = coefficients ranging from 0.784 - 0.641; $p < 0.008$). To estimate the temporary progression of functional recovery per rat,

a score was obtained per animal by summing the level achieved each month during 8 months posttransplantation. We selected this period because there was no further improvement after the seventh month. The final score obtained for each rat in the performance in the climbing test correlated with both the total number of labeled cell bodies ($r = 0.897$; $p < 0.001$) and the number of somata in each nucleus ($r = 0.899$-0.847; $p < 0.001$). These positive linear correlations are consistent with the concept that these brainstem neurons contributed to the functional improvement of the implanted rats. In addition, there was a linear negative correlation between the volume of GFAP-negative tissue (fibrosis and cavities) and the total number of traced brainstem neurons in both, all ($r = -0.767$ $p < 0.001$) and each ($r = 0.780$-0.697; $p < 0.002$) nuclei. This indicates that the smaller the degenerative events at the injury site, the greater axonal regeneration across. Therefore, our results suggest a role of OB-OEG on tissue preservation and/or tissue formation at the lesion zone that may facilitate axonal regeneration across.

DISCUSSION

The OB-OEG promoted both functional recovery of paraplegic rats and regeneration of supraspinal axons caudal to the lesion in rats receiving a graft after 1 and 4 months after the complete lesion. Strikingly, functional outcome after OB-OEG transplantation at 4 months post-lesion did not differ from that at either SA or acute (4) time points. In addition, axonal regeneration of brainstem neurons, involved in different aspects of motor function (34), was more than twice in OB-OEG-transplanted versus nontransplanted rats, again, with no differences related to time posttransplantation. Finally, the positive correlation between locomotor performance and extent of axonal regeneration distally is consistent with those brainstem neurons having contributed to the motor recovery (35-37). Thus, our results show that the effectiveness of adult OB-

OEG and tissue repair was not affected by the stage of the scarring processes, and that injured neurons preserved their capacity to positively respond to OB-OEG for at least 4 months.

The beneficial effects of OB-OEG have been related to enhanced axonal regeneration, survival and tissue sparing, remyelination, stimulation of angiogenesis and neuroprotection (38-41). Moreover, a recent report revealed that OB-OEG express key molecules involved in the response to wounding, blood vessel development, extracellular matrix formation and remodelling, and cell adhesion (42). Based on the present results, therefore, OB-OEG transplantation at subacute and chronic SCI stages could be exerting a reparative action via any or all of the mechanisms; remyelination was not examined in this study, however.

Our study constitutes the first evidence showing that chronic SCI can be repaired by OEG transplants. Lu et al (19) and Lopez-Vales et al (20) performed transplantation at the subacute stage, that is, after 30 and 45days, respectively. Moreover, we used adult OB-OEG (central), whereas in the former OEG were obtained from lamina propria (peripheral) and in the latter study, from neonatal bulbs. It has been reported that mucosal OEG do not exhibit the same migratory or axonal growth-promoting properties as bulbar OEG in rodents (16-18) and neonatal OEG do not exhibit the same properties as adult (24-43). The observation that implantation of adult OEG can improve recovery after spinal cord injury and a decrease in efficacy when used in a chronic stage makes this a more realistic paradigm for autologous cell therapy for chronic SCI.

In the context of a possible future clinical application, it has been demonstrated that OEG can be obtained from the OBsof adult humans (44) and non-human primates (11). These cells can be easily cultured in standard incubators and expanded in large numbers just using serum-containing medium. A culture of one single primate olfactory

bulb provides, in a short term (ten days *in vitro*), around 1.5-2 million OEG, and additional 20 billion cells after 2.5 months. This large number guarantees not only autologous transplantation but also provides cells for allotransplantation and storage. These cells express similar axonal-growth related molecules as rodent cells *in vitro* (11, 44) A key issue in this regard is the demonstration that primate OB-OEG from healthy donors ranging in age from 1.5 to 10 years (young to mature adult), promoted locomotor recovery after transplantation into paraplegic rodents (45). The surgical procedures that are compatible with human practice for unilateral bulbectomy and for autologous transplantation into injured spinal cords have been determined and checked for safety in non-human primates (11, 27). Therefore, these data point to the OB as a reliable source of OEG for cell therapy.

A remaining and important issue addressed in the present study was the feasibility of OB-OEG autologous grafting for spinal cord repair. The most probable clinical scenario is of a young adult or adult patient who requires stabilization of the clinical condition after accident. Hence, it seems safer to perform bulbectomy some time after injury. Moreover, after bulb removal, cells need to be grown for at least 10 days in order to obtain enough OEG for transplantation. Accordingly, the experimental condition that would mimic the clinical situation more closely is the implantation in the chronic situation of OEG obtained from adults. We show that adult OB-OEG can effectively promote functional recovery and repair in paraplegic mammals when they are transplanted at chronic stages. Grafting can be delayed for, at least, a period of 4 months postlesion with no decrease in beneficial effects. In the case of an autologous therapy, this window would seem to provide enough time to obtain and prepare OEG from the olfactory bulbs and also for patient stabilization before the surgery. Therefore,

our results open the prospect for a future therapy with autologous implanted OB-OEG in patients experiencing a severe chronic SCI.

Acknowledgements

The authors thank Prof. V Reggie Edgerton from UCLA for his contribution to improve the quality of the article. We are grateful to Luisa Juan and Natividad Pozo for help in animal care and Nuria Ruiz for providing support and advice for statistical analyses.

REFERENCES

1. Franssen EH, de Bree FM, Verhaagen J. Olfactory ensheathing glia: their contribution to primary olfactory nervous system regeneration and their regenerative potential following transplantation into the injured spinal cord. Brain Res Rev 2007;56:236-58.
2. Ramon-Cueto A, Nieto-Sampedro M. Regeneration into the spinal cord of transected dorsal root axons is promoted by ensheathing glia transplants. Exp Neurol 1994;127:232-44.
3. Ramon-Cueto A, Plant GW, Avila J, et al. Long-distance axonal regeneration in the transected adult rat spinal cord is promoted by olfactory ensheathing glia transplants. J Neurosci 1998;18:3803-15.
4. Ramon-Cueto A, Cordero MI, Santos-Benito FF, et al. Functional recovery of paraplegic rats and motor axon regeneration in their spinal cords by olfactory ensheathing glia. Neuron 2000;25:425-35.
5. Imaizumi T, Lankford KL, Waxman SG, et al. Transplanted olfactory ensheathing cells remyelinate and enhance axonal conduction in the demyelinated dorsal columns of the rat spinal cord. J Neurosci 1998;18:6176-85.
6. Nash HH, Borke RC, Anders JJ. Ensheathing cells and methylprednisolone promote axonal regeneration and functional recovery in the lesioned adult rat spinal cord. J Neurosci 2002;22:7111-20.
7. Li Y, Decherchi P, Raisman G. Transplantation of olfactory ensheathing cells into spinal cord lesions restores breathing and climbing. J Neurosci 2003;23:727-31.
8. Verdu E, Garcia-Alias G, Fores J, et al. Olfactory ensheathing cells transplanted in lesioned spinal cord prevent loss of spinal cord parenchyma and promote functional recovery. Glia 2003;42:275-86.
9. Ruitenberg MJ, Levison DB, Lee SV, et al. NT-3 expression from engineered olfactory ensheathing glia promotes spinal sparing and regeneration. Brain 2005;128:839-53.
10. Plant GW, Christensen CL, Oudega M, et al. Delayed transplantation of olfactory ensheathing glia promotes sparing/regeneration of supraspinal axons in the contused adult rat spinal cord. J Neurotrauma 2003;20:1-16.
11. Rubio MP, Munoz-Quiles C, Ramon-Cueto A. Adult olfactory bulbs from primates provide reliable ensheathing glia for cell therapy. Glia 2008;56:539-51.
12. Barakat DJ, Gaglani SM, Neravetla SR, et al. Survival, integration, and axon growth support of glia transplanted into the chronically contused spinal cord. Cell Transplant 2005;14:225-40.
13. Collazos-Castro JE, Muneton-Gomez VC, Nieto-Sampedro M. Olfactory glia transplantation into cervical spinal cord contusion injuries. J Neurosurg Spine 2005;3:308-17.
14. Pearse DD, Sanchez AR, Pereira FC, et al. Transplantation of Schwann cells and/or olfactory ensheathing glia into the contused spinal cord: Survival, migration, axon association, and functional recovery. Glia 2007;55:976-1000.
15. Resnick DK, Cechvala CF, Yan Y, et al. Adult olfactory ensheathing cell transplantation for acute spinal cord injury. J Neurotrauma 2003;20:279-85.
16. Ramer LM, Richter MW, Roskams AJ, et al. Peripherally-derived olfactory ensheathing cells do not promote primary afferent regeneration following dorsal root injury. Glia 2004;47:189-206.

17. Lu P, Yang H, Culbertson M, et al. Olfactory ensheathing cells do not exhibit unique migratory or axonal growth-promoting properties after spinal cord injury. J Neurosci 2006;26:11120-30.
18. Steward O, Sharp K, Selvan G, et al. A re-assessment of the consequences of delayed transplantation of olfactory lamina propria following complete spinal cord transection in rats. Exp Neurol 2006;198:483-99.
19. Lu J, Feron F, Mackay-Sim A, et al. Olfactory ensheathing cells promote locomotor recovery after delayed transplantation into transected spinal cord. Brain 2002;125:14-21.
20. Lopez-Vales R, Fores J, Navarro X, et al. Chronic transplantation of olfactory ensheathing cells promotes partial recovery after complete spinal cord transection in the rat. Glia 2007;55:303-11.
21. Hill CE, Beattie MS, Bresnahan JC. Degeneration and sprouting of identified descending supraspinal axons after contusive spinal cord injury in the rat. Exp Neurol 2001;171:153-69.
22. Velardo MJ, Burger C, Williams PR, et al. Patterns of gene expression reveal a temporally orchestrated wound healing response in the injured spinal cord. J Neurosci 2004;24:8562-76.
23. Kubasak MD, Jindrich DL, Zhong H, et al. OEG implantation and step training enhance hindlimb-stepping ability in adult spinal transected rats. Brain 2008;131:264-76.
24. Ramon-Cueto A, Avila J. Olfactory ensheathing glia: properties and function. Brain Res Bull 1998;46:175-87.
25. Cahi E, Rosen M, Becker PJ. A comparison of the dimensional stability of three inlay pattern materials. J Dent Assoc S Afr 1996;51:337-42.
26. McDonnell T, Houston F, Byrne D, et al. The effect of time lapse on the accuracy of two acrylic resins used to assemble an implant framework for soldering. J Prosthet Dent 2004;91:538-40.
27. Santos-Benito FF, Munoz-Quiles C, Ramon-Cueto A. Long-term care of paraplegic laboratory mammals. J Neurotrauma 2006;23:521-36.
28. Iannotti C, Ping Zhang Y, Shields CB, et al. A neuroprotective role of glial cell line-derived neurotrophic factor following moderate spinal cord contusion injury. Exp Neurol 2004;189:317-32.
29. Oorschot DE. Are you using neuronal densities, synaptic densities or neurochemical densities as your definitive data? There is a better way to go. Prog Neurobiol 1994;44:233-47.
30. Paxinos G, Watson C. The rat brain in stereotaxic coordinates. Fourth edition. San Diego California: Academic Press, 1998.
31. Agresti A. Categorical Data Analysis. Second edition. Florida: Wiley-Interscience, 2002.
32. Moses LE, JD. Hosseini, H. Analyzing data from ordered categories. Second edition. Boston: New England Journal of Medicine, 1992.
33. Conover W. Practical Nonparametric Statistics. Third edition: Wiley, 1999.
34. Tracey DJ. Ascending and descending pathways in the spinal cord. In: G P ed. The rat nervous system, Vol. Primary afferent projections to the spinal cord. San Diego: Academic Press, 1995:67-75.
35. Courtine G, Bunge MB, Fawcett JW, et al. Can experiments in nonhuman primates expedite the translation of treatments for spinal cord injury in humans? Nat Med 2007;13:561-6.

36. Metz GA, Merkler D, Dietz V, et al. Efficient testing of motor function in spinal cord injured rats. Brain Res 2000;883:165-77.
37. Whishaw IQ, Gorny B, Sarna J. Paw and limb use in skilled and spontaneous reaching after pyramidal tract, red nucleus and combined lesions in the rat: behavioral and anatomical dissociations. Behav Brain Res 1998;93:167-83.
38. Woodhall E, West AK, Chuah MI. Cultured olfactory ensheathing cells express nerve growth factor, brain-derived neurotrophic factor, glia cell line-derived neurotrophic factor and their receptors. Brain Res Mol Brain Res 2001;88:203-13.
39. Boruch AV, Conners JJ, Pipitone M, et al. Neurotrophic and migratory properties of an olfactory ensheathing cell line. Glia 2001;33:225-9.
40. Barnett SC, Riddell JS. Olfactory ensheathing cell transplantation as a strategy for spinal cord repair--what can it achieve? Nature clinical practice 2007;3:152-61.
41. Richter MW, Roskams AJ. Olfactory ensheathing cell transplantation following spinal cord injury: hype or hope? Exp Neurol 2008;209:353-67.
42. Franssen EH, De Bree FM, Essing AH, et al. Comparative gene expression profiling of olfactory ensheathing glia and Schwann cells indicates distinct tissue repair characteristics of olfactory ensheathing glia. Glia 2008;56:1285-98.
43. Barnett SC. Olfactory ensheathing cells: unique glial cell types? J Neurotrauma 2004;21:375-82.
44. Barnett SC, Alexander CL, Iwashita Y, et al. Identification of a human olfactory ensheathing cell that can effect transplant-mediated remyelination of demyelinated CNS axons. Brain 2000;123:1581-8.
45. Guest JD, Herrera L, Margitich I, et al. Xenografts of expanded primate olfactory ensheathing glia support transient behavioral recovery that is independent of serotonergic or corticospinal axonal regeneration in nude rats following spinal cord transection. Exp Neurol 2008;212:261-74.
46. Keyvan-Fouladi N, Raisman G, Li Y. Functional repair of the corticospinal tract by delayed transplantation of olfactory ensheathing cells in adult rats. J Neurosci 2003;23:9428-34.
47. Liu HS, Jan MS, Chou CK, et al. Is green fluorescent protein toxic to the living cells? Biochem Biophys Res Commun 1999;260:712-17.
48. Detrait ER, Bowers WJ, Halterman MW, et al. Reporter gene transfer induces apoptosis in primary cortical neurons. Mol Ther 2002;5:723-30.
49. Torbett BE. Reporter genes: too much of a good thing? J Gene Med 2002;4:478-79.
50. Doi K, Hargitai J, Kong J, et al. Lentiviral transduction of green fluorescent protein in retinal epithelium: evidence of rejection. Vision Res 2002;42:551-58
51. Dusart I, Marty S, Peschanski M. Glial changes following an excitotoxic lesion in the CNS--II. Astrocytes. Neuroscience 1991;45:541-49.
52. Lakatos A, Barnett SC, Franklin RJ. Olfactory ensheathing cells induce less host astrocyte response and chondroitin sulphate proteoglycan expression than Schwann cells following transplantation into adult CNS white matter. Exp Neurol 2003;184:237-46.

Appendix 1

Climbing Test

For this test, a rat has to climb from a grid of 25 x 25-mm^2 holes and completely pass its body onto a smooth horizontal platform located at a height of 70 cm. The platform is smooth and slippery so the animals cannot cross it using their forelimbs. An animal can only succeed if it voluntarily moves its hindlimbs, properly placing the paws on the rungs and pushing its body upward (Video, Supplemental Digital Content 1, http://links.lww.com/NEN/A62). The test has 4 difficulty levels (i.e. 1-4) depending on the slope of the grid (45, 60, 75, or 90 degrees, respectively). The higher the slope, the greater body weight support. Normal uninjured rats (and shams) achieve the highest level. To motivate the animals, they were rewarded with chocolate-hazelnut cream after each good performance. All animals were within a similar range of weight (270-300 g) for comparisons. Each animal was allowed 10 attempts per session. An attempt was counted when the rats pushed with their forelimbs and propelled the head above the horizontal platform. To keep animals unable to achieve the test motivated, a grid with 1 x 1-cm squares on top of the smooth platform was placed only after several unsuccessful tries. Using this grid, animals could pull with the forelimbs upward, complete the performance, and receive the reward (Video, Supplemental Digital Content 1, http://links.lww.com/NEN/A62). We only considered a positive result when a rat achieved a specific level during 3 different weeks. Three examiners blinded to the treatment evaluated the outcome at the time of testing and by reviewing the videotapes of the sessions.

Video sequences of the last part of the performances of representative Non-T rats and OB-OEG-grafted rats (SA and Chr) are shown (Video, Supplemental Digital

Content 1, http://links.lww.com/NEN/A62). The first video sequence is an example of a Non-T rat trying to achieve the lowest climbing level. This rat was unable to use its hindlimbs voluntarily and could not propel the body onto the smooth horizontal platform. A surface with a grid was placed on top of the platform so the animal could reach the top and be rewarded after unsuccessful attempts. The second video sequence shows an OB-OEG-transplanted rat achieving Level 1 at 4 months after grafting. This animal improved later on and achieved higher climbing levels. The third sequence shows an OB-OEG-grafted rat accomplishing the maximum level reached, that is, Level 3. The 3 sequences are shown in slow motion to demonstrate hindlimb voluntary movements in transplanted rats compared with their absence in the Non-T animal.

Appendix 2

Tracking and Distribution of Grafted OB Ensheathing Glia After Transplantation

There are no good markers for long-term detection of OB-OEG. Most of the immunocytochemical markers used for OEG detection in vitro may cause misleading results in vivo because they also label other cells. For example, anti-p75 antibody does not discriminate between grafted OEG and endogenous Schwann cells invading the lesion (7, 46). Transduction of OEG by adenoviruses or lentiviruses encoding tag molecules could be used to track transplanted OEG, but genetic manipulation of the cells may change their phenotype. For long-term transplantation studies, the expression of genetic markers should be stable for the entire survival period, and the tag molecule should be nontoxic. Green fluorescent protein has been used in shorter-term transplantation studies to identify OB-OEG, but stable expression occurs only for up to 4 months (1); thus, it is inappropriate for our experimental paradigm. Moreover, other

studies report toxic effects of green fluorescent protein on some cell types (47-49); some of these were not evident in culture but appeared after transplantation (50).

In view of these data and our need to track the fate of OB-OEG 8 months after transplantation, we labeled the cells with bisbenzimide (Hoechst 33342; Sigma-Aldrich Química), as in our previous studies (3, 4). To our knowledge, this is the only vital dye that lasts 8 months after transplantation and has no toxic effects on OB-OEG. To be certain that the dye was not transferred from OEG to other cells, we determined whether the dye was present in macrophages immunostained with the anti-CD68 antibody ED1 (Serotec MCA341R; 1:100) in the lesion sites of transplanted rats by confocal microscopy. The same sections were labeled with either anti-GFAP to delimit glial and fibrous scars (51, 52) or anti-S100 to detect OB-OEG (24). This analysis was performed on 10% of all spinal cord sections that were equally separated by 200 Km from 4 transplanted rats, using a Leica confocal microscope (DM IRE2).

The GFAP immunohistochemistry delimits glial and fibrous scars created at the injury site (Figure, Supplemental Digital Content 3, http://links.lww.com/NEN/A64, part A). We detected numerous Hoechst-labeled cells at both fibrous and glial scars (Figure, Supplemental Digital Content 3, http://links.lww.com/NEN/A64, parts A and B). There were few ED1-positive macrophages that were mainly located at the glial scar and borders of the fibrous scar (Figure, Supplemental Digital Content 3, http://links.lww.com/NEN/A64, parts A and C). If leakage of bisbenzimide had occurred from prelabeled OB-OEG, macrophages should have had blue nuclei, but we did not observe colocalization of ED1 and Hoechst dye within the same cells, indicating that the dye was not transferred to phagocytic cells (Figure, Supplemental Digital Content 3, http://links.lww.com/NEN/A64, parts B-D). Hence, if the dye had not been

phagocytosed by macrophages, it is very unlikely that it was transferred fromOB-OEG to other cells that lack active phagocytic activity.

Fibrous scars created after SCI are formed by fibroblasts and are devoid of astrocytes; hence, they are GFAP and S100 negative (51, 52) (Figure, Supplemental Digital

Content 3, http://links.lww.com/NEN/A64, part A). The OBOEG express S100 (24), and an antibody against this molecule can be used to identify OB-OEG in the fibrous scars of transplanted cords. S100-positive OB-OEG were found within the fibrous scar (Figure, Supplemental Digital Content 3, http://links.lww.com/NEN/A64, part E), and Hoechst-labeling colocalized with them (Figure, Supplemental Digital Content 3, http://links.lww.com/NEN/A64, part F). The absence of Hoechst uptake by macrophages and the identification of this marker in OB-OEG indicate that under our experimental conditions, OB-OEG can be identified by their Hoechst nuclear staining.

Hoechst-labeled OB-OEG migrated from the injection sites and invaded the glial scars at both rostral and caudal stumps, and also the fibrous scar. They intermingled with reactive astrocytes and the inhibitory environment of the fibrous scar tissue did not hinder their migration (Figure, Supplemental Digital Content 3, http://links.lww.com/NEN/A64, parts A and B). Some OB-OEG could also be found at the rostral and caudal spinal cord stumps. The OB-OEG seemed to properly integrate within the host parenchyma because there was neither swelling of the tissue, phagocytic cells around grafted OB-OEG, nor tissue disruption at the sites of injection that would suggest graft rejection. The histological appearance of the stumps was indistinguishable from that of sham control cords.

FIGURE 1

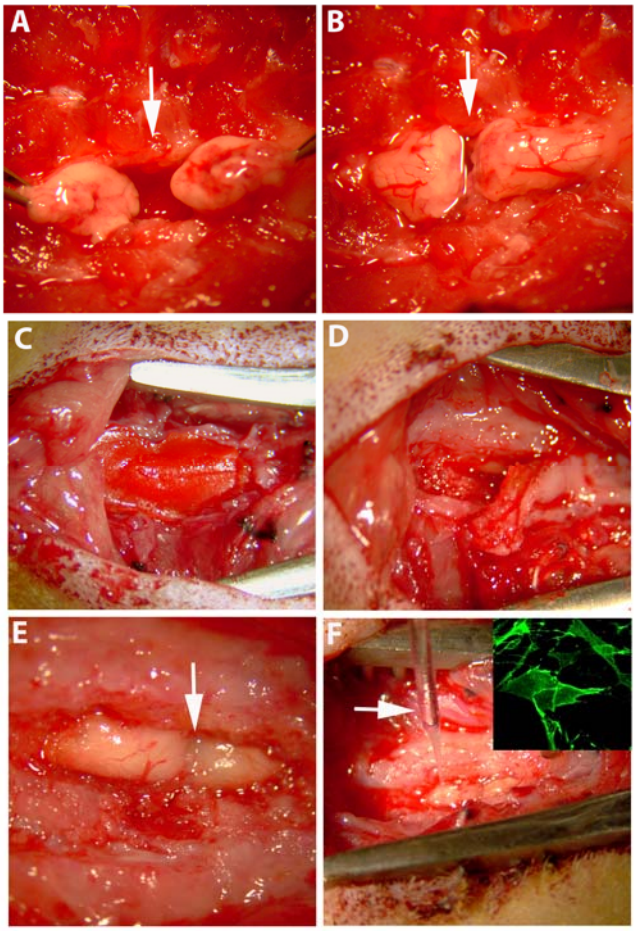

Figure 1. Appearance of the surgical field during different phases of the procedure. A. After transection, both spinal cord stumps were lifted to ensure completeness of the lesion. **B**. Spinal cord stumps were placed back into the vertebral channel, apposing one another. **C-F** shows the aspect of the lesion region during the second surgery (access to the spinal cord for transplantation). **C**. We first found the resin bridge (arrow) firmly sealed to the spinous processes and laminae of adjacent intact vertebrae. **D**. After bridge removal, we found a dense layer of connective tissue that was removed (arrowheads) to expose the spinal cord underneath (arrow). **E**. Dorsal aspect of both spinal cord stumps, four months after complete transection. **F**. Transplantation of OB-OEG using a glass micro-needle (pointed by an arrow). Inbox shows a detail of an OB-OEG culture used for transplantation and immunolabelled against p75. Arrow in A, B and E points to the spinal cord transection site.

FIGURE 2

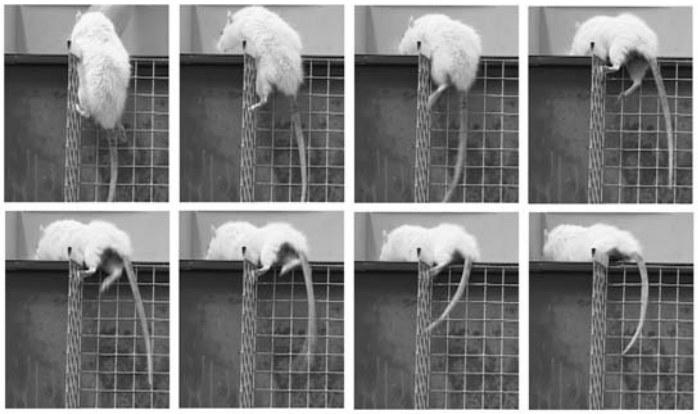

Figure 2. Video frames showing a paraplegic rat transplanted with OB-OEG at the chronic stage, achieving the third climbing level, five months after transplantation. We show a detail of the hind limb movement of this rat supporting its weight, and propelling the body to reach the horizontal platform. The video of this animal is provided as Supplemental data file 2.

FIGURE 3

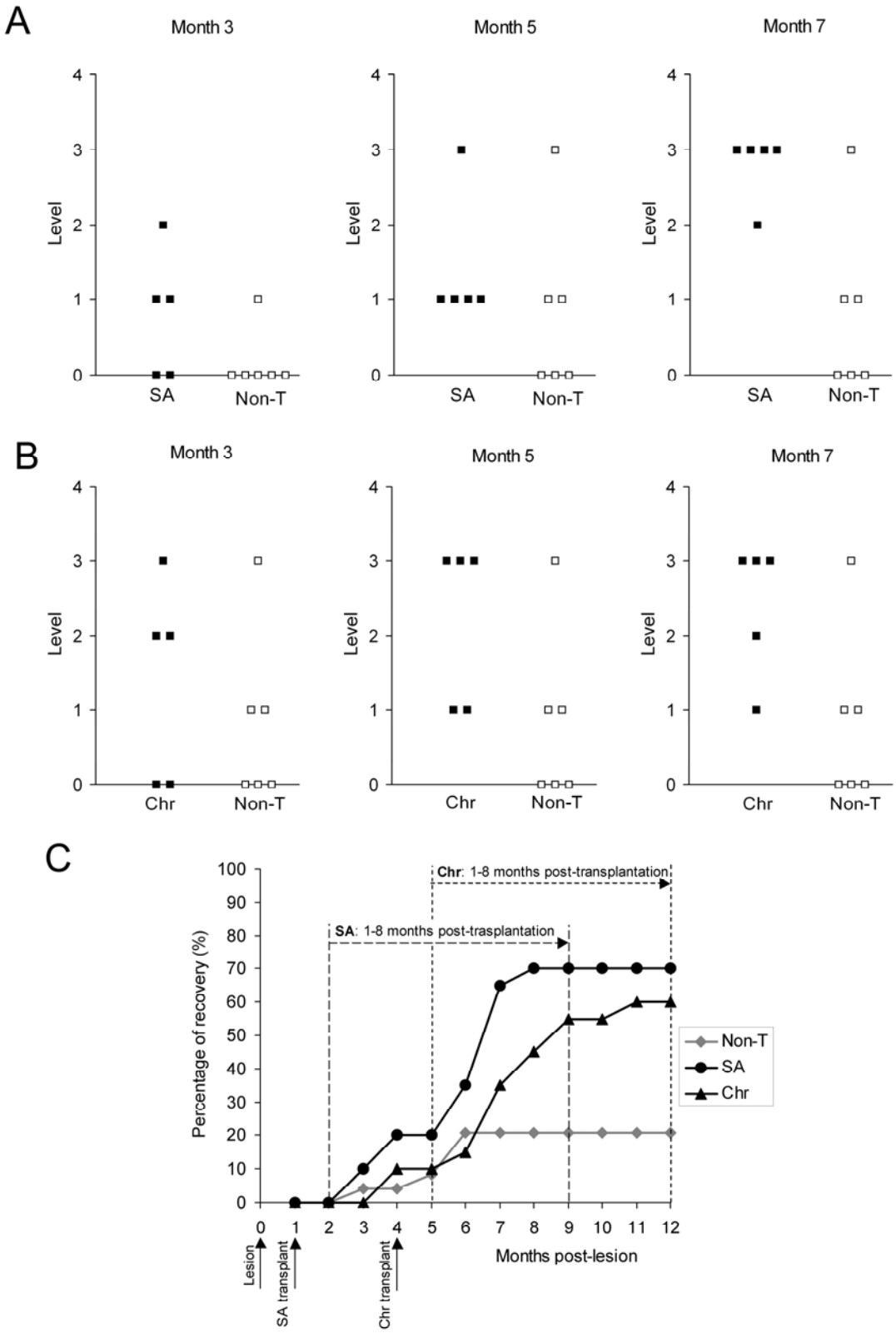
A
Month 3
Month 5
Month 7
Level
SA
Non-T
B
Chr
C
Chr: 1-8 months post-transplantation
SA: 1-8 months post-trasplantation
Percentage of recovery (%)
Months post-lesion
Lesion
SA transplant
Chr transplant
Non-T
SA
Chr

Figure 3. Functional recovery of paraplegic rats after OB-OEG transplantation at subacute (SA) and chronic (Chr) stages. A, B. Levels achieved in the climbing test by (**A**) non-transplanted (Non-T) and SA, and by (**B**) Non-T and Chr rats, at 3, 5 and 7 months post-grafting.

Transplanted rats showed a functional recovery significantly higher than Non-T (SA: $p < 0.001$ and Chr: $p = 0.001$). Differences started to be significant from month six in SA rats (month 6: $p = 0.029$, month 7 and 8: $p = 0.020$), and from month seven in Chr ($p = 0.045$). There were no differences between SA and Chr groups (compare A and B). C. Progression of the functional outcome in all groups from the first month post-lesion until the end of the survival period (month twelve). Each point represents the percentage of functional recovery exhibited by animals of each group. Dashed lines show the periods we used to compare the outcome of Non-T versus SA (long dash) and Non-T versus Chr animals (short dash) from the first till the eighth month post-grafting. Non-T animals (grey rhombs) showed a slight but not significant recovery. Before grafting, Chr and SA groups behaved as Non-T animals. SA group (black circles) and Chr (black triangles) started improving two months after OB-OEG transplantation (three and six months post-lesion, respectively). Improvement of SA and Chr rats commenced at the second month, and began to be significant from the fifth ($p=0.004$) and four months ($p=0.021$) respectively.

FIGURE 4

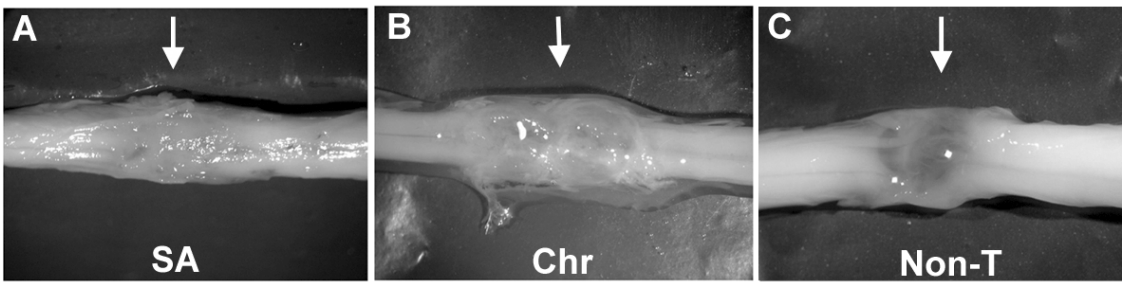

Figure 4. Aspect of the transection site of OB-OEG-grafted and non-transplanted spinal cords, twelve months after lesion. Representative macroscopic images of spinal cords from (**A**) SA and (**B**) Chr OB-OEG transplanted rats, and from (**C**) one Non-T rat. In all transplanted spinal cords (SA and Chr), rostral and caudal stumps were bridged by a white and opaque tissue (A and B), whereas in Non-T rats cord stumps were joined by a translucent membrane (C).

FIGURE 5

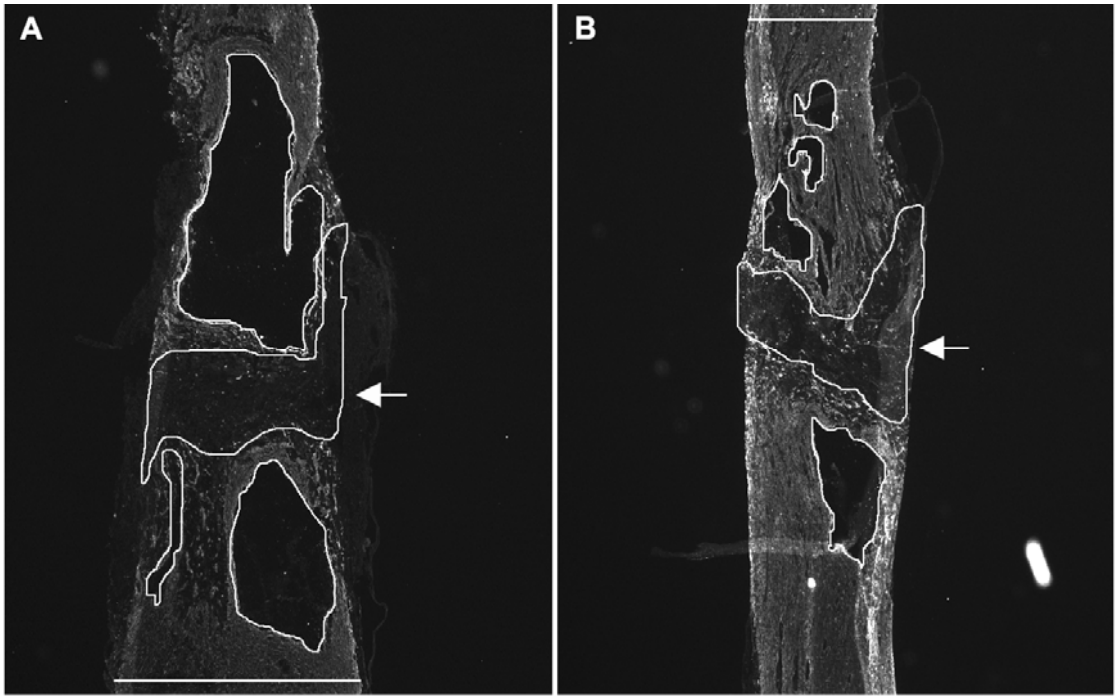

Figure 5. Longitudinal spinal cord sections showing the areas used for quantification of GFAP negative tissue at the injury site. Sections of Non-T (**A**) and OB-OEG-transplanted (**B**) spinal cords, immunolabelled with anti-GFAP. Encircled lines represent both, GFAP negative fibrous scar (pointed by arrows) and cysts (without arrows). The width of the cords for each individual animal was also measured in the sections (horizontal lines in A and B). Top: rostral; bottom: caudal.

FIGURE 6

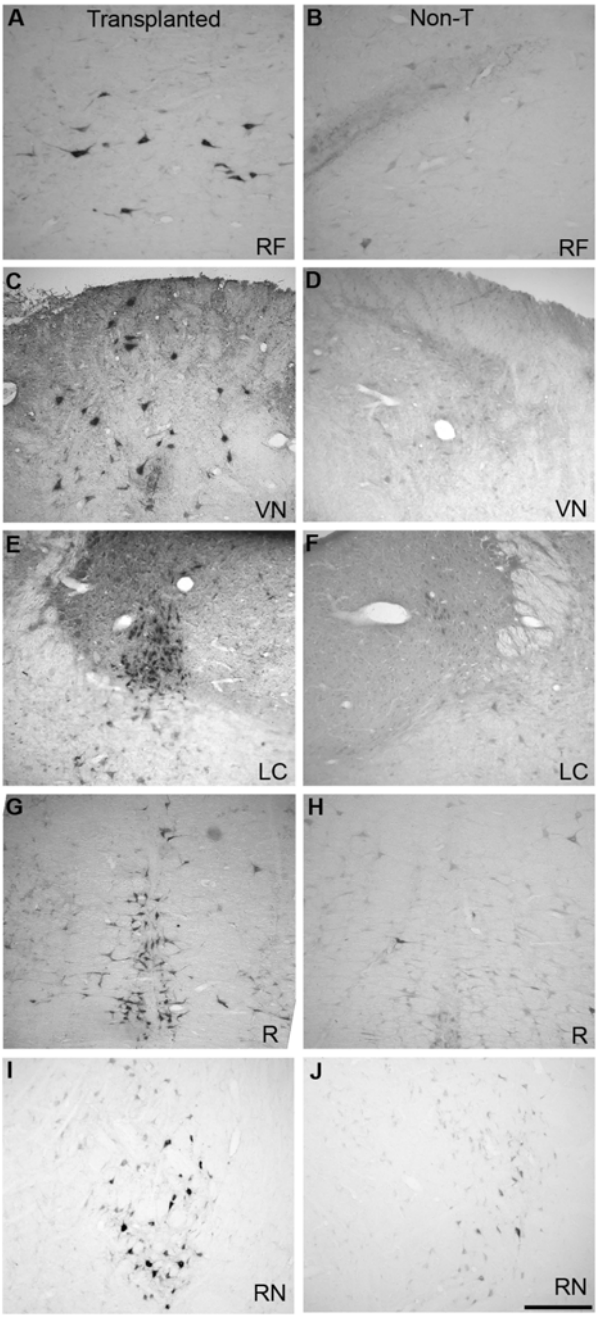

Figure 6. Brainstem coronal sections showing peroxidase-traced neurons in OB-OEG-transplanted (A, C, E, G, I) and non-transplanted (B, D, F, H, J) rats. **A**, **B**, reticular formation (RF). **C**, **D**, vestibular nucleus (VN). **E**, **F**, locus coeruleus (LC). **G**, **H**, raphe (R). **I**, **J**, red nucleus (RN). Panels on the left show sections from OB-OEG transplanted rats and those on the right correspond to Non-T rats. Scale bar **A-J** = 50 μm. Top: dorsal; bottom: ventral.

FIGURE 7

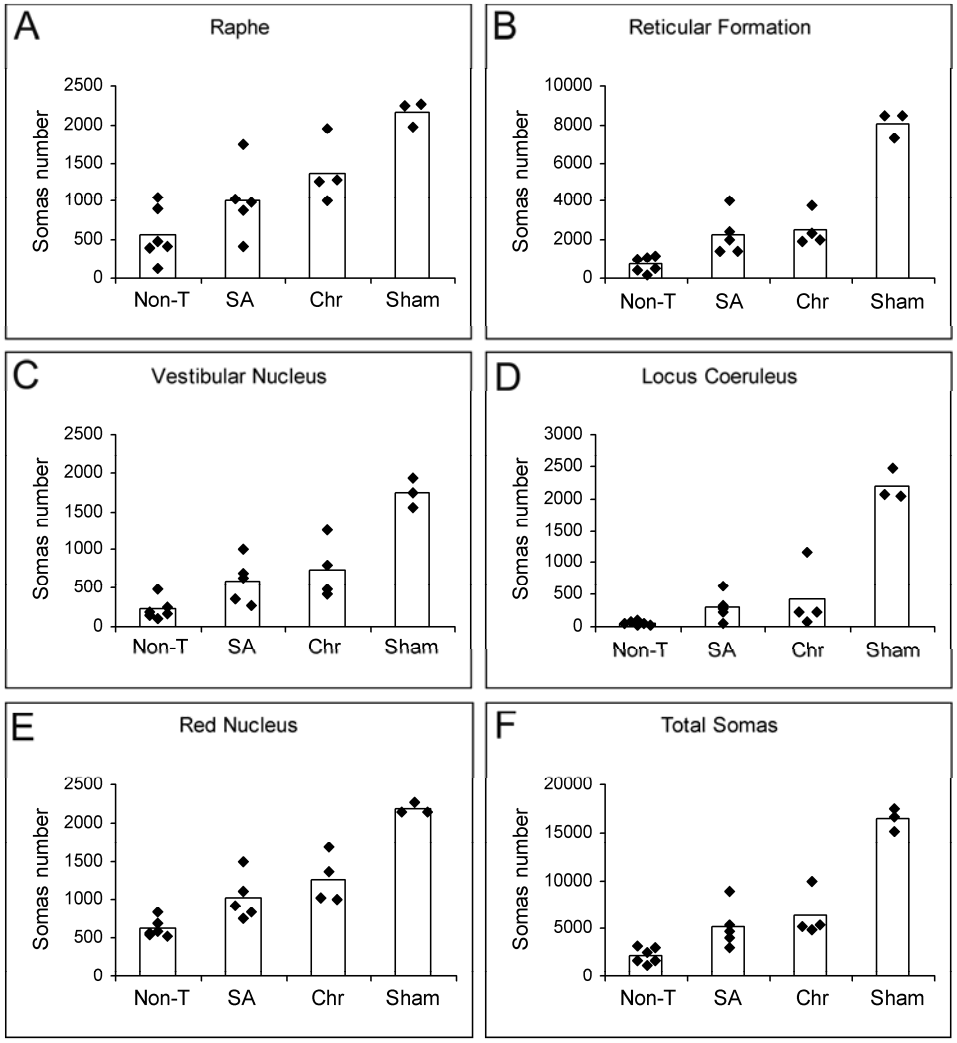

Figure 7. Quantification of neurons regenerating axons beyond the injury region. A-E. Histograms show the number of peroxidase-traced neurons in Non-T, SA, Chr and Sham groups counted in raphe (A), reticular formation (B), vestibular nuclei (C), locus coeruleus (D), red nuclei (E), and in all nuclei (F). Black rhombs represent the number of cell bodies per animal and bars the average of cell bodies per group. The total number of traced neurons was significantly higher in SA and Chr animals than in Non-T, and also when comparing per nuclei (except for raphe in SA rats) ($p < 0.05$). There were not significant differences between SA and Chr groups in any case.

TABLE

	Rafe		F. Reticular		N. Vestibular		L. Coeruleus		N. Rojo		TOTAL	
GROUPS	**somas**	%	**somas**	%	**somas**	%	**somas**	%	**somas**	%	**somas**	%
Sham	2167 ± 81	100	8107 ± 338	100	1740 ± 94	100	2202 ± 120	100	2183 ± 40	100	16399 ± 609	100
SA	1009 ± 240	47	2273 ± 528	28	593 ± 143	34	303 ± 107	14	1025 ± 145	47	5203 ± 1116	32
Cr	1373 ± 200	63	2522 ± 430	31	746 ± 193	43	418 ± 249	19	1271 ± 161	58	6330 ± 1176	39
No-T	561 ± 171	26	730 ± 202	9	224 ± 69	13	53 ± 14	2	631 ± 61	29	2198 ± 416	14

Table 1. Number of peroxidase-containing neurons in the brainstems of Sham, SA, Chr and Non-T animals. Data are presented as mean ± SEM. This table also shows the percentage of labeled neurons per nuclei and per group. We considered as 100% the average of labeled neurons in sham animals.

SUPPLEMENTAL DIGITAL CONTENT 1

Figure Legend_Supplemental Data File 1_Movie file.

We show some video sequences of the last part of the performances of representative Non-T rats and OB-OEG grafted rats (SA and Chr). The first sequence of this movie is an example of a Non-T rat trying to achieve the lowest climbing level. This rat was unable to voluntary use its hindlimbs and could not propel the body onto the smooth horizontal platform. To avoid demotivation of animals unable to climb (such as Non-T rats), and only after several tries, a gridded surface was placed on top of the platform, so the animals can reach the top and be rewarded. But this was never done unless animals made tries.

The second video sequence shows an example of one OB-OEG-transplanted rat achieving level 1, four months after grafting. Details of hindlimb movement and how the animal placed the paws on the rungs can be seen in slow motion. This animal improved later on and achieved higher climbing levels. The third sequence shows one OB-OEG-grafted rat accomplishing the maximum level reached: level 3. All three sequences are shown in slow motion to better visualize hindlimb voluntary movement of transplanted rats compared to the absence of this Non-T animals.

SUPPLEMENTAL DIGITAL CONTENT 2

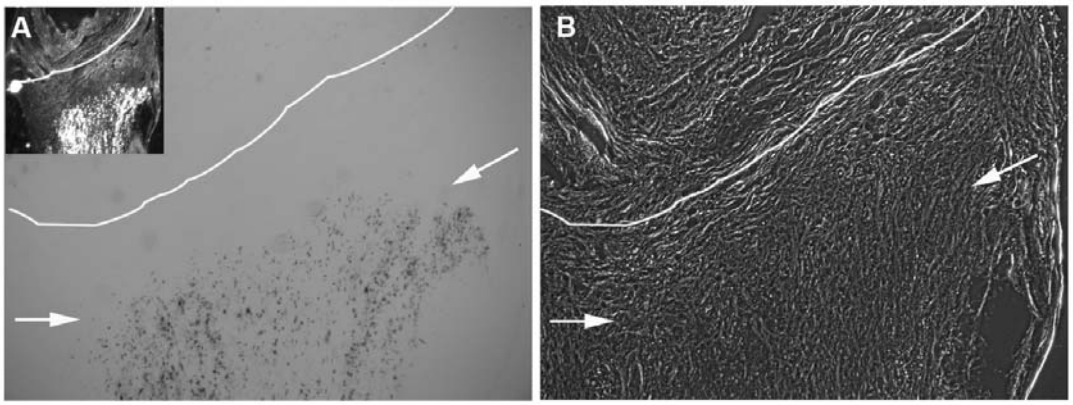

Figure Legend_Supplemental Data File 2_Figure.

Tracer did not diffuse from the injection site into the injury region and remained beyond within the caudal spinal cord stump. All three pictures show the same field of the caudal spinal cord stump, visualized using (A) bright field, (B) phase contrast, and dark field (inbox in A). Arrows point to tracer location in the caudal spinal cord stump. Dashed lines delimit the caudal border of the injury. Notice that the tracer remained within the caudal stump and did not invade the injury region.

SUPPLEMENTAL DIGITAL CONTENT 3

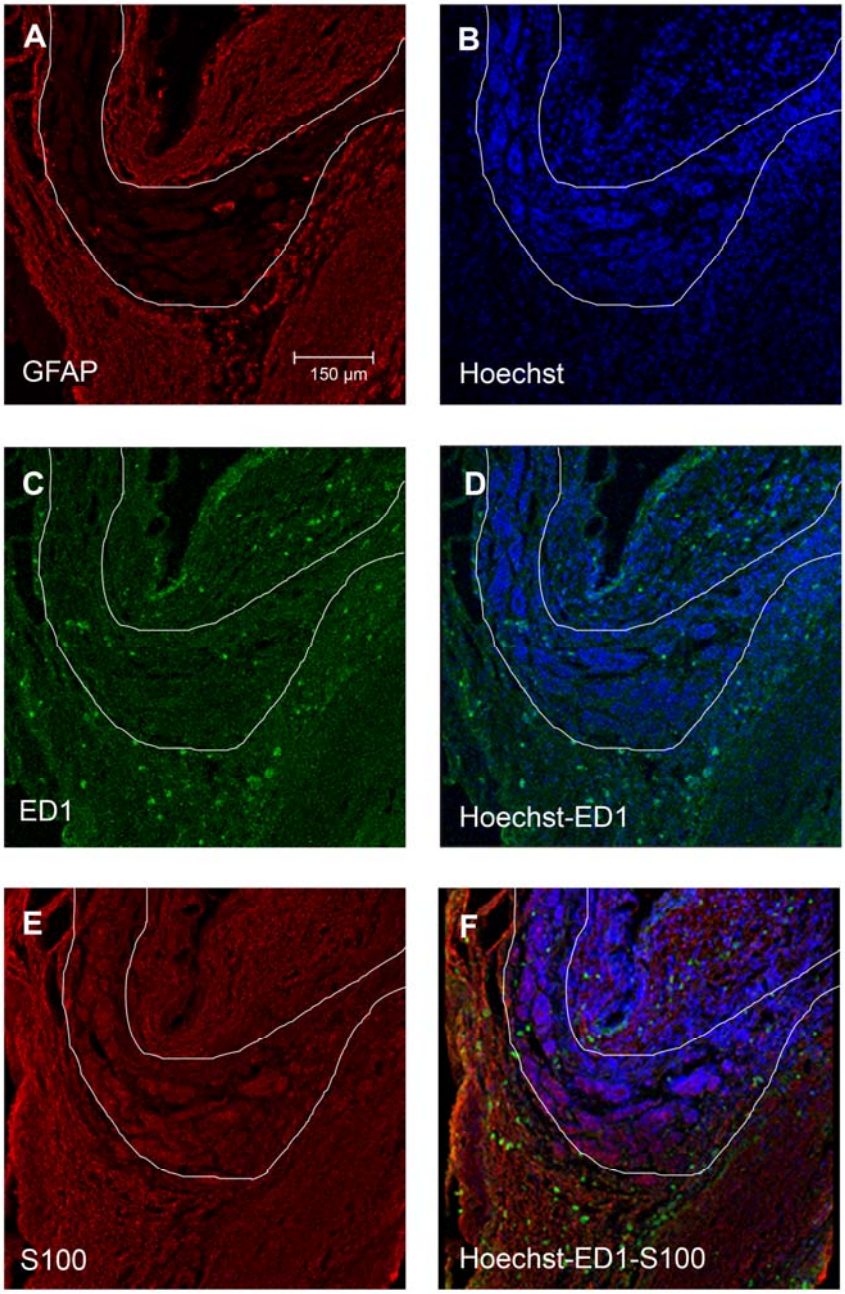

Figure Legend Appendix 2

Confocal microscopy images of the spinal cord injury region eight months after OB-OEG transplantation at chronic stage. Final images are the merge of the confocal images (stacks) obtained from each whole section. **A-D** show the same filed of a section immunostained with anti-GFAP and ED1. **E-F** panels represent an adjacent

section to that shown in A-D, immunostained against S100 and ED1. **A**, GFAP positive immunoreactivity delimits the glial and the fibrous scars. **B**, Visualization of Hoechst labeled OB-OEG in the same section shown in A. **C,** Immunostaining of macrophages and microglia in the same section using anti-ED1 antibody. **D**, Merge of B and C. ED1 positive macrophages (green) were not labelled with Hoechst (blue). **E** shows S100 positive cells in the fibrous scar (compare A and E). **F.** Cells stained with anti-S100 (red), anti-ED1 (green) and Hoechst (blue). Notice in the fibrous scar the presence of cells expressing S100 and labeled with Hoechst. White line in all the figures encircles the fibrous scar. Scale bar in all figures= 150 μm.